Title

Molecular Identification and Functional Characterization of the Human Colonic Thiamine Pyrophosphate Transporter*

Journal

Journal of Biological Chemistry, 289(7)

ISSN

0021-9258

Authors

Nabokina, Svetlana M
Inoue, Katsuhisa
Subramanian, Veedamali S
et al.

Publication Date

2014-02-01

DOI

10.1074/jbc.m113.528257

THE JOURNAL OF BIOLOGICAL CHEMISTRY VOL. 289, NO. 7, pp. 4405–4416, February 14, 2014
Published in the U.S.A.

Molecular Identification and Functional Characterization of the Human Colonic Thiamine Pyrophosphate Transporter*

Received for publication, October 17, 2013, and in revised form, December 13, 2013 Published, JBC Papers in Press, December 30, 2013, DOI 10.1074/jbc.M113.528257

Svetlana M. Nabokina[‡§], Katsuhisa Inoue[¶], Veedamali S. Subramanian[‡§], Judith E. Valle[‡§], Hiroaki Yuasa[‖], and Hamid M. Said[‡¶1]

From the [‡]Departments of Medicine and Physiology/Biophysics, University of California, Irvine, California 92697, the [§]Department of Veterans Affairs Medical Center, Long Beach, California 90822, the [¶]Department of Biopharmaceutics, School of Pharmacy, Tokyo University of Pharmacy and Life Sciences, Tokyo 192-0392, Japan, and the [‖]Department of Biopharmaceutics, Graduate School of Pharmaceutical Sciences, Nagoya City University, Nagoya 467-8603, Japan

Background: Human colonocytes possess a specific, high-affinity, and regulated carrier-mediated system for TPP uptake.
Results: Human SLC44A4 protein functions as a TPP transporter.
Conclusion: The SLC44A4-mediated TPP uptake system may play a role in the absorption of the microbiota-generated TPP in colon.
Significance: Molecular identification of the colon-specific TPP uptake system is important for understanding the mechanisms of overall thiamine nutrition.

Colonic microbiota synthesize a considerable amount of thiamine in the form of thiamine pyrophosphate (TPP). Recent functional studies from our laboratory have shown the existence of a specific, high-affinity, and regulated carrier-mediated uptake system for TPP in human colonocytes. Nothing, however, is known about the molecular identity of this system. Here we report on the molecular identification of the colonic TPP uptake system as the product of the *SLC44A4* gene. We cloned the cDNA of SLC44A4 from human colonic epithelial NCM460 cells, which, upon expression in ARPE19 cells, led to a significant ($p < 0.01$, >5-fold) induction in [^{3}H]TPP uptake. Uptake by the induced system was also found to be temperature- and energy-dependent; Na^+-independent, slightly higher at acidic buffer pH, and highly sensitive to protonophores; saturable as a function of TPP concentration, with an apparent K_m of 0.17 ± 0.064 μM; and highly specific for TPP and not affected by free thiamine, thiamine monophosphate, or choline. Expression of the human TPP transporter was found to be high in the colon and negligible in the small intestine. A cell surface biotinylation assay and live cell confocal imaging studies showed the human TPP transporter protein to be expressed at the apical membrane domain of polarized epithelia. These results show, for the first time, the molecular identification and characterization of a specific and high-affinity TPP uptake system in human colonocytes. The findings further support the hypothesis that the microbiota-generated TPP is absorbable and could contribute toward host thiamine homeostasis, especially toward cellular nutrition of colonocytes.

Thiamine (vitamin B_1) is an essential micronutrient that is required by all living organisms for critical metabolic pathways, including oxidative (sugar) metabolism, mitochondrial ATP synthesis, and reduction of cellular oxidative stress. In these reactions, thiamine (mainly in its diphosphorylated form, TPP[2]) acts as a cofactor for the involved enzymes (reviewed in Refs. 1, 2). Deficiency of thiamine in humans leads to serious clinical abnormalities that include neurological and cardiovascular disorders. Such a deficiency occurs in chronic alcoholics, diabetic patients, and other at-risk groups (3–6).

All mammals, including humans, have an absolute requirement for exogenous thiamine because they lack the ability to synthesize the vitamin *de novo*. Two sources of thiamine are available to humans: a dietary source and a bacterial source. Dietary thiamine exists mainly in the form of TPP, which is hydrolyzed to free thiamine by the abundant small intestinal phosphatases prior to absorption (3, 4, 7). Liberated free thiamine is then taken up by the polarized enterocytes via a specific carrier-mediated process that involves both thiamine transporters 1 and 2 (THTR-1 and THTR-2; in humans, these systems are referred to as hTHTR-1 and hTHTR-2) (3, 4, 7).

Regarding the bacterial source of thiamine, the microbiota of the large intestine produce a significant amount of both free and phosphorylated (TPP) forms of the vitamin (8–11). In fact, a recent study that has shown that the human gut microbiota exist in three functionally different enterotypes (enterotypes 1, 2, and 3) has reported that enterotype 2 (which is enriched in *Prevotella* and *Desulfovibrio*) is characteristically enriched in enzymes that are involved in the biosynthesis of TPP (8). We have shown previously that human colonocytes are capable of taking up free thiamine via a specific and highly efficient pro-

* This work was supported, in whole or in part, by National Institutes of Health Grant DK 56061-15 (to H. M. S.). This work was also supported by the Department of Veteran Affairs (to H. M. S.).

[1] To whom correspondence should be addressed: Veterans Affairs Medical Center-151, Long Beach, CA 90822. Tel.: 562-826-5811; Fax: 562-826-5675; E-mail: hmsaid@uci.edu.

[2] The abbreviations used are: TPP, thiamine pyrophosphate; THTR, thiamine transporter; TPPT, TPP transporter; hTPPT, human TPP transporter; MDCK, Madin-Darby canine kidney; BBM, brush border membrane; qRT-PCR, quantitative RT-PCR; TM, transmembrane; CTL, choline transporter-like; FCCP, carbonyl cyanide *p*-trifluoromethoxyphenylhydrazone; CCCP, carbonyl cyanide *m*-chlorophenylhydrazone; DIDS, 4,4′-diisothiocyanostilbene-2,2′-disulfonic acid; SITS, 4-acetamido-4′-isothiocyanostilbene-2,2′-disulfonic acid; ABC transporter, ATP-binding cassette transporter.

cess (12) similar to the one that functions in the small intestine (reviewed in Refs. 3, 4).

As for the microbiota-generated TPP, it has been assumed that human colonocytes are unable to take up this form of the vitamin because of its size, charge, and hydrophilic nature and the fact that colonocytes have little or no surface alkaline phosphatase activity (13–15). However, recent functional studies from our laboratory that utilized non-transformed human colonic epithelial NCM460 cells and native human colonic apical membrane vesicles from human organ donors as well as custom-made [^{3}H]TPP have shown, for the first time, the existence of a specific, highly efficient, and regulated carrier-mediated process for [^{3}H]TPP uptake (16). Nothing, however, is known about the molecular identity of the system involved, its characteristics, and the pattern of its distribution in different tissues and cell types. We addressed these issues in this study and report here that the colonic TPP transporter (TPPT, hTPPT for humans) is a product of the *SLC44A4* gene. We successfully cloned the hTPPT from human colonic epithelial NCM460 cells and characterized its function following expression in human retinal pigment epithelial ARPE19 cells. Our studies showed a predominant expression of this transporter in the colon, with little expression in other parts of the gastrointestinal tract. Finally, the TPPT was found to display a predominant expression at the apical membrane domain of epithelia. These findings represent the first molecular identification of a human uptake system that is specific for TPP and suggest that this system may play a role in the absorption of microbiota-generated TPP in the large intestine.

EXPERIMENTAL PROCEDURES

Materials—The NCM460 cell line was from INCELL (San Antonio, TX). ARPE19 and Madin-Darby canine kidney (MDCK) cells were purchased from the ATCC. Custom-made ^{3}H-labeled thiamine pyrophosphate ([^{3}H]TPP; specific activity, 1.0 Ci/mmol; radiochemical purity, 98.3%) was obtained from Moravek Biochemicals, Inc. (Brea, CA). Unlabeled TPP, TMP, and thiamine were purchased from Sigma. The pFLAG-CMV-2 vector was from Sigma. The YFP-N1 fluorescent protein vector was from Clontech (Mountain View, CA). The Human Major Tissue qPCR Panel II was from OriGene (Rockville, MD). Isolated and purified human jejunal brush border membrane (BBM) and colonic apical membrane (AM) preparations were provided by Dr. P. K. Dudeja (University of Illinois at Chicago) and were prepared as described previously (17, 18) in accordance with the institutional protocols approved by the Institutional Review Board of the University of Illinois at Chicago. All other chemicals and reagents were purchased from commercial sources and were of analytical grade.

Bioinformatic Searches for the hTPPT and Its Isolation—The protein-protein basic local alignment search tool (BLASTP) algorithm and the SOSUI and TMHMM transmembrane helix prediction programs were used in our searches for mammalian homologs of the TPP ABC transporter permease (TDE0144, accession number NP_970761) of the oral spirochete *Treponema denticola* (19). Our search has led to the identification of SLC44A4 as the potential candidate. Searching the NCBI database, we found three alternatively spliced transcript variants of the human *SLC44A4*, *i.e.* transcript variants 1, 2, and 3 (accession numbers NM_025257, NM_001178044, and NM_001178045, respectively), which encode protein isoforms 1, 2, and 3, respectively. We cloned variants 1 and 3 because they were the only two variants found to be expressed in human colonic epithelial cells (see "Results"). The human SLC44A4 cDNAs of variants 1 and 3 (designated hTPPT-1 and hTPPT-3, respectively) were isolated by RT-PCR using mRNA from human colonic NCM460 cells and specific primers. The mRNA from NCM460 cells was prepared with a NucleoTrap mRNA Midi kit (Clontech) following the protocol of the manufacturer, and a first-strand cDNA mixture was made from 0.5 μg of mRNA primed with oligo(dT) using the Superscript II synthesis system (Invitrogen). The hTPPT-1- and hTPPT-3-specific cloning primers were as follows: hTPPT-1, 5′-ATGGGGGGAAAGCAGCGGGACGAG-3′ (forward) and 5′-TCACTTCTTCCTCTTCTTGTTG-3′ (reverse); hTPPT-3, 5′-ATGGGGGAGAACAAAGATAAGCCGTATC-3′ (forward) and 5′-TCACTTCTTCCTCTTCTTGTTG-3′ (reverse). The PCR was performed with Advantage 2 polymerase mix (Clontech) using the following conditions: denaturation at 95 °C for 3 min followed by 33 cycles of denaturation at 95 °C for 1 min, annealing at 55 °C for 1 min, extension at 72 °C for 3 min, and then a final extension at 72 °C for 10 min. The PCR products were cloned into the pGEM-T Easy vector (Promega, Madison, WI), and the DNA sequences were verified by the Laragen Sequencing Facility (Los Angeles, CA).

The ORFs of hTPPT-1 and hTPPT-3 were then subcloned into the expression plasmid pFLAG-CMV-2 using the HindIII and BamHI sites. The primers used for subcloning into pFLAG-CMV-2 were as follows: hTPPT-1, 5′-AAAAGCTTATGGGGGGAAAGCAGCGGGACGAG-3′ (forward) and 5′-GGGGATCCTCACTTCTTCCTCTTCTTGTTG-3′; and hTPPT-3, 5′-GGAAGCTTATGGGGGAGAACAAAGATAAGCCGTATC-3′ (forward) and 5′-GGGGATCCTCACTTCTTCCTCTTCTTGTTG-3′ (reverse). The HindIII and BamHI sites are *underlined*. The ORF of hTPPT-1 was subcloned into the yellow fluorescent protein YFP-N1 vector (Clontech) using the HindIII and SacII sites and the following primer combinations: 5′-AAAAGCTTATGGGGGGAAAGCAGCGGGACGAG-3′ (forward) and 5′-TCCCCGCGGCTTCTTCCTCTTCTTGTT-3′ (reverse). The HindIII and SacII sites are *underlined*. The DNA sequences were verified by the Laragen Sequencing Facility.

Cell Culture and Transfection—Cells were maintained in DMEM (ARPE19 cells) or minimum Eagle's medium (MDCK cells) supplemented with 10% (v/v) FBS, penicillin (100,000 units/liter), and streptomycin (10 mg/liter). NCM460 cells were maintained in Ham's F-12 culture medium supplemented with 20% (v/v) FBS and antibiotics.

For uptake studies, ARPE19 cells were grown on 12-well tissue culture plates (Corning, NY). For imaging studies, MDCK cells were grown on sterile glass-bottomed Petri dishes (MatTek, Ashland, MA). At ~90% confluence, cells were transfected with 2 μg of plasmid DNA with Lipofectamine 2000 (Invitrogen). 48 h after transfection, cells were used for uptake assays (with RNA and protein measurements done in parallel) or analyzed by confocal microscopy.

TPP Uptake Studies—Uptake studies were performed on confluent ARPE19 cell monolayers 48 h following transfection as described previously (16). Briefly, cells were incubated in Krebs-Ringer buffer containing 133 mM NaCl, 4.93 mM KCl, 1.23 mM $MgSO_4$, 0.85 mM $CaCl_2$, 5 mM glucose, 5 mM glutamine, 10 mM HEPES, and 10 mM MES (pH 7.4 unless stated otherwise) at 37 °C for 3 min (the initial linear period; uptake was found to be linear for up to 10 min of incubation (data not shown)). [^{3}H]TPP (0.3 μM unless stated otherwise) was added to the incubation medium at the onset of uptake experiment, and the reaction was terminated after 3 min by the addition of ice-cold Krebs-Ringer buffer, followed by immediate aspiration and washings. Cells were lysed with 1 ml of 1 N NaOH, lysates were neutralized with HCl, and then radioactivity was assessed using a Beckman Coulter LS6500 multipurpose scintillation counter (Fullerton, CA). Protein was measured in parallel using a Bio-Rad DC protein assay kit (Bio-Rad).

Quantitative Real-time PCR Analysis—Total RNA (2 μg) was isolated from various human-derived cell lines and distinct segments of mouse intestine, followed by a reverse transcription reaction using an iScript cDNA synthesis kit (Bio-Rad) to generate first-strand cDNAs to be used in qRT-PCR. The Human Major Tissue qPCR Panel II (OriGene), containing PCR-ready, first-strand cDNAs, was also used in the qRT-PCR. The mRNA of the hTPPT and mouse TPPT expression level was quantified in a CFX96 real-time PCR system (Bio-Rad) using iQ SYBR Green Supermix (Bio-Rad). Primers were as follows: hTPPT, 5′-TGCTGATGCTCATCTTCCTGCG-3′ (forward) and 5′-GGACAAAGGTGACCAGTGGGTA-3′ (reverse); mouse TPPT, 5′-TGCCTACCAGAGTGTGAAGGAG-3′ (forward) and 5′-TGGCTTCCTTCAGCAGAGCGAT-3′ (reverse); human GAPDH, 5′-GTCTCCTCTGACTTCAACAGCG-3′ (forward) and 5′-ACCACCCTGTTGCTGTAGCCAA-3′ (reverse); and mouse GAPDH, 5-CATCACTGCCACCCAGAAGACTG-3′ (forward) and 5′-ATGCCAGTGAGCTTCCCGTTCAG-3′ (reverse). Real-time PCR conditions were as described previously (20), and data were normalized to GAPDH and then quantified using a relative relationship method supplied by the iCycler manufacturer (Bio-Rad).

PCR and Semiquantitative PCR Analysis—Total RNA (2 μg) was isolated from NCM460 cells, followed by a reverse transcription reaction using an iScript cDNA synthesis kit (Bio-Rad). The PCR primers were designed on the basis of the sequence information for transcript variants 1, 2, and 3 in GenBank™ (accession numbers NM_025257, NM_001178044, and NM_001178045, respectively) and were as follows: hTPPT-1, 5′-ATCACTCCGGAGACTGAGCC-3′ (forward) and 5′-TACCCCTGGCAGACAAAAGT-3′ (reverse); hTPPT-3, 5′-CTGGGGTTGACACCTTTGTCT-3′ (forward) and 5′-CCCCAACAGTCTGTGAGAACT-3′ (reverse); and hTPPT-1/hTPPT-2, 5′-GTCTCCAGGGCTCCAATCAC-3′ (forward) and 5′-GTTCCTGTTGCAGGCTTGTG-3′ (reverse). Control GAPDH-specific primers were as follows: 5′-ACCACAGTCCATGCCATCAC-3′ (forward) and 5′-TCCACCACCCTGTTGCTGTA-3′ (reverse). The PCR was performed with Advantage 2 polymerase mix (Clontech) using the following conditions: denaturation at 95 °C for 3 min, denaturation at 95 °C for 0.5 min, annealing at 60 °C for 0.5 min, and extension at 72 °C for 0.5 min (35 cycles for PCR and 18–30 cycles (linear range) for semiquantitative PCR), followed by analysis of the PCR products on 2% agarose gels.

Western Blot Analysis—Proteins (whole cell lysates, biotinylated proteins, or colonic apical membrane preparations) were separated in NuPAGE 4–12% Bis-Tris gradient minigels (Invitrogen), transferred onto Immobilon polyvinylidene difluoride membranes (Fisher Scientific), and subjected to Western blot analysis. The primary antibodies were rabbit polyclonal anti-hTPPT/SLC44A4 antibodies (CTL4 (D-14) antibody, catalog no. sc-68049, Santa Cruz Biotechnology, Santa Cruz, CA) at 1:200 dilution. The secondary antibody was anti-rabbit IRDye-800 antibody at 1:30,000 dilution. Immunoreactive bands were visualized using the Odyssey infrared imaging system (LI-COR Bioscience).

Cell Surface Protein Biotinylation—Biotinylation of cell surface proteins in NCM460 cells was performed with a cell surface protein isolation kit (Pierce) following the protocol of the manufacturer. Briefly, cells were labeled with EZ-Link Sulfo-NHS-SS-Biotin, lysed, and then the biotinylated proteins were isolated with NeutrAvidin-agarose. The bound proteins were released with NuPAGE lithium dodecyl sulfate sample buffer and analyzed by Western blotting using anti-hTPPT/SLC44A4 antibodies (CTL4 (D-14) antibody, Santa Cruz Biotechnology).

Live Cell Confocal Imaging—Transfected MDCK cell monolayers were imaged using an inverted Nikon C-1 confocal microscopy 48 h post-transfection. The YFP was excited with a 488-nm laser line, and the emitted fluorescence was monitored at 515 ± 30 nm with a short pass filter. Images were captured with Nikon C-1 software (Nikon Instruments Inc., NY).

TLC—Mouse colonic mucosal homogenate (~1 mg of total protein in 250 μl of Krebs-Ringer buffer (pH 7.4)) was incubated with [^{3}H]TPP (0.6 μM) at 37 °C for up to 2 h, followed by identification of the forms of ^{3}H radioactivity by TLC, as described previously (16, 21). Mouse studies were approved by the Long Beach, Veteran Affairs Subcommittee on Animal Studies. Briefly, 15 μl of 100% trichloroacetic acid was added to the reaction mixture, followed by centrifugation and extraction with water-saturated ethyl ether. The TLC-ready purified sample was mixed with unlabeled thiamine, TMP, and TPP (1 mM each, final concentration), applied onto the TLC plate (20 × 20-cm plate coated with a 250-μm layer of silica gel, Whatman), and run using a solvent system of diethanolamine:methanol: formic acid-67 mM dibasic sodium phosphate (1:15:1.5:5). The separation of thiamine derivatives was checked under UV light. Pieces of silica gel corresponding to thiamine, TMP, and TPP were cut, and radioactivity was assessed using a Beckman Coulter LS6500 multipurpose scintillation counter.

Data Presentation and Statistical Analysis—The data of uptake experiments are presented as mean ± S.E. of multiple individual uptake determinations and are expressed in picomoles per milligram of protein per unit of time. The uptake of TPP by the induced system was calculated by subtracting the uptake by ARPE19 cells transfected with SLC44A4 from the uptake by ARPE19 cells transfected with an empty vector. Student's *t* test was used in statistical analysis, with statistical significance set at $p < 0.01$ or $p < 0.05$. Kinetic parameters of the saturable TPP uptake process (*i.e.* maximal velocity (V_{max}) and

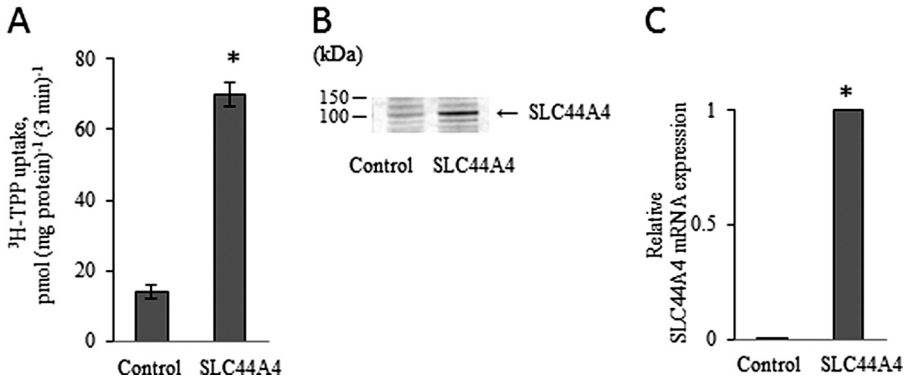

FIGURE 1. **The SLC44A4 protein functions as a TPP transporter.** ARPE19 cells were transiently transfected with the ORF of human *SLC44A4* (hTPPT-1), followed 48 h later by measurement of [^{3}H]TPP uptake and determination of the hTPPT expression level. *A*, initial rate of [^{3}H]TPP uptake by ARPE19 cells. Cells were incubated at 37 °C in Krebs-Ringer buffer (pH 7.4). [^{3}H]TPP (0.3 μM) was added to the incubation medium at the onset of incubation, and uptake was measured after 3 min (*i.e.* initial rate) of incubation. Data are the mean ± S.E. of at least five independent experiments with three to four separate uptake determinations. *B*, Western blot analysis was performed using ~80 μg of protein from the cell lysates. The blot was probed with the polyclonal antibodies directed against hTPPT. The image is from a representative set of experiments. *C*, total RNA was isolated, and real-time quantitative PCR was performed. Data (means ± S.E.), normalized relative to GAPDH, are from three independent experiments. Note that the mean for the control is not visible on the scale of the graph. In all experiments, control cells were transiently transfected with the empty pFLAG-CMV-2 vector. *, $p < 0.01$.

the apparent Michaelis-Menten constant (K_m)) were calculated as described by Wilkinson (22). Uptake by the saturable component was calculated at each concentration by subtracting the uptake by simple diffusion (determined from the slope of the line between the point of origin and the uptake at a high concentration of TPP (1 mM) from the total uptake). All Western blot analyses, the biotinylation assay, PCR assays, and confocal imaging studies were performed on two or more separate occasions with similar results.

RESULTS

Identification of the hTPPT—Basic Local Alignment Search Tool (BLAST) searches for mammalian homologs of the recently identified TPP ABC transporter permease (TDE0144, accession number NP_970761) of the oral spirochete *T. denticola* (19) were performed to delineate the molecular identity of the human colonic TPP uptake system (16). With the use of the BLASTP algorithm and the transmembrane helix prediction programs, *i.e.* SOSUI and TMHMM, one protein (the product of the *SLC44A4* gene, accession number NP_079533) was found to have a significant similarity to the partial amino acid sequence of TPP ABC transporter permease in regions that are predicted to be in substrate-binding domains. The substrate-binding domain prediction for the TPP ABC transporter permease was made on the basis of the available data of x-ray crystallography of Mhp1, a bacterial transporter for sodium-benzylhydantoin, which proposes that the substrate-binding site of Mhp1 consists of transmembrane (TM) segments TM1, TM2, TM6, and TM7 (23). Using the TDE0144 amino acid sequence corresponding to the TM1, TM2, TM6, and TM7 segments as a query in our BLASTP homology searches, we found that the 272–370 amino acid region of the SLC44A4 polypeptide reveals a low but significant degree of homology (26% of identity and 49% of similarity) with the query sequence. The identified candidate for the mammalian TPP transporter represents an uncharacterized multitransmembrane protein with unknown function. On the basis of its amino acid sequence, however, the SLC44A4 protein has been placed in the family of choline transporter-like (CTL) proteins and originally annotated as choline transporter-like protein 4 (CTL4, reviewed in Ref. 24).

We found three alternatively spliced variants of human *SLC44A4*, *i.e.* transcript variants 1, 2, and 3 (accession numbers NM_025257, NM_001178044, and NM_001178045, respectively), listed in the NCBI database, which encode protein isoforms 1, 2, and 3, respectively. In this report, we cloned variants 1 and 3 but focused our characterization on variant 1 because it showed the highest level of expression in human colonic epithelial cells compared with variant 3 (there was no expression of variant 2 in these cells) (see below). We successfully cloned the ORF of the *SLC44A4* variant 1 into the expression plasmid pFLAG-CMV-2 using mRNA from human colonic NCM460 cells and primers specific for that variant. The generated construct was then used for transient transfection of human retinal epithelial ARPE19 cells followed by determination of [^{3}H]TPP uptake. A significant ($p < 0.01$) and marked (about 5-fold) induction in [^{3}H]TPP uptake (0.3 μM) was found in cDNA-transfected cells compared with control (vector-transfected) cells (Fig. 1*A*). This induction in TPP uptake was found to be associated with the parallel induction in expression of SLC44A4 at the protein (Fig. 1*B*) and mRNA (Fig. 1*C*) levels. A Western blot analysis performed with the specific polyclonal anti-SLC44A4 antibodies (for description of the antibodies, see "Experimental Procedures") (Fig. 1*B*) resulted in the detection of the prominent immunoreactive band of ~110 kDa in ARPE19 cells transiently expressing SLC44A4. In contrast, this protein band was found to be of a very low intensity in control ARPE19 cells expressing endogenous SLC44A4. The observed immunoreactive band is likely to represent the glycosylated form of the SLC44A4 protein (the predicted molecular mass of SLC44A4 protein variant 1 is 79.2 kDa).

These findings (together with the findings on specificity described below) allowed us to conclude that the SLC44A4 protein is indeed a TPPT. In further work outlined in this report, the human SLC44A4 variant 1 and hTPPT-1 were used interchangeably.

Structural Features of the hTPPT-1—The ORF of hTPPT-1 encodes a protein of 710 amino acids. The predicted molecular mass and pI of the protein is 79,254 Da and 8.91, respectively. A comparison of the deduced amino acid sequence of hTPPT-1 with those of various mammalian species (Fig. 2*A*) using BLAST reveals a high degree of homology (*i.e.* 82–86% of identity) between the proteins, indicating that the TPPT is highly conserved across mammals. As for being originally assigned to the choline transporter-like family, which contains choline transporter-like proteins 1–5 encoded by the *SLC44A1–5* genes (24), hTPPT-1 (originally annotated as CTL-4) shows a considerable amino acid similarity with human CTL2 and CTL5 (52 and 46%, respectively).

A hydrophobicity analysis using SOSUI predicted that the hTPPT-1 protein contains 13 putative transmembrane domains and displays an extracellular amino terminus and an intracellular carboxyl terminus (Fig. 2*B*). According to this topographical model, there is one potential *N*-linked glycosylation site (Asn^{29}), which is located in the extracellular N terminus. Putative intracellular loops contain consensus sequences for phosphorylation by protein kinase C (Ser^{169}), Ca^{2+}/calmodulin-dependent protein kinase (Ser^{304} and Thr^{406}), and tyrosine kinase (Tyr^{58}, Tyr^{280}, Tyr^{302}, Tyr^{387}, Tyr^{685}, and Tyr^{686}).

Functional Characteristics of hTPPT-1—Functional characterization of hTPPT-1 was performed in ARPE19 cells transiently transfected with FLAG-hTPPT-1. Uptake by the induced hTPPT-1 was determined as described under "Experimental Procedures." The results showed the induced uptake (3 min, initial rate) of [^{3}H]TPP (0.3 μM) by SLC44A4-expressing ARPE19 cells to be temperature-dependent because a significant ($p < 0.01$) decrease in uptake was found upon lowering the incubation temperature from 37 to 22 °C (58.89 ± 4.33 and 31.69 ± 1.02 pmol (mg protein/3 min) for 37 °C and 22 °C, respectively). The induced [^{3}H]TPP uptake was also energy-dependent because significant ($p < 0.01$) inhibition occurred as a result of pretreatment (for 30 min) of the SLC44A4-expressing cells with the metabolic inhibitor 2,4-dinitrophenol (1 mM) (50.42 ± 4.85 and 27.37 ± 3.62 pmol (mg protein/3 min) for the control and following pretreatment with 2,4-dinitrophenol, respectively).

Dependence of the induced [^{3}H]TPP uptake in SLC44A4-expressing ARPE19 cells on availability of Na^+ in incubation medium was determined by examining the effect of isosmotically replacing Na^+ (133 mM) in the incubation medium with the monovalent cation Li^+ (133 mM) or with the inert mannitol (266 mM) on initial rate of [^{3}H]TPP (0.3 μM) uptake at pH 7.4. The results (Fig. 3*A*) showed no significant effect of replacing Na^+ with either Li^+ or mannitol on hTPPT-1-specific TPP uptake. These data indicate that Na^+ is not involved in uptake of TPP by the induced system.

Dependence of the induced TPP uptake in SLC44A4-expressing cells on the availability of H^+ in the incubation medium was determined by examining the effect of varying the buffer pH. The results (Fig. 3*B*) showed that, although uptake by the induced TPP uptake system does not display a clear pH optimum within the examined range of pH (5.0–9.0), it was found to be slightly but significantly ($p < 0.01$) higher at an acidic pH of 5.0 compared with that at an alkaline pH of 8.5–9.0. In another study, we examined the effect of pretreating (for 20 min) ARPE19 cells with the protonophores carbonyl cyanide *p*-trifluoromethoxyphenylhydrazone (FCCP, 10 μM) and carbonyl cyanide *m*-chlorophenylhydrazone (CCCP, 10 μM) on the initial rate of [^{3}H]TPP (0.3 μM) uptake by the induced system. The results (Fig. 3*C*) showed that both protonophores caused a significant ($p < 0.01$) inhibition in TPP uptake by the induced system. Indeed, the uptake was decreased by ~76 and 85% by FCCP and CCCP, respectively. Proton ionophores were not included in the incubation buffer at the time of uptake determinations, and, thus, direct competitive inhibition of TPP uptake by these compounds was not the case. These findings suggest a role for the inwardly directed H^+ gradient in TPP uptake by the SLC44A4-mediated system and raise the possibility of the involvement of a TPP^--H^+ cotransport mechanism. Further studies are required to address this issue.

TPP is an organic anion. Therefore, it was interesting to examine whether any of the membrane transport inhibitors (*i.e.* probenecid and the stilbene disulphonate derivatives DIDS and SITS) that typically act on the transport of anionic substrates are capable to affect TPP uptake by the induced system. It was also of interest to assess the ability of amiloride, another membrane transport inhibitor that has been shown previously to inhibit the uptake of free thiamine in a variety of cellular systems, including human intestinal epithelial cells (25), to inhibit TPP uptake by the induced system. Therefore, we examined the effect of the above mentioned membrane transport inhibitors (all at 0.5 mM) on the uptake of [^{3}H]TPP (0.3 μM) by the induced system in SLC44A4-expressing ARPE19 cells. The uptake was found to be significantly ($p < 0.01$) inhibited by all tested compounds (54.84 ± 3.02, 20.7 ± 0.79, 8.76 ± 0.67, 12.01 ± 1.08, and 34.08 ± 2.19 pmol (mg protein/3 min) for the control, probenecid, DIDS, SITS, and amiloride, respectively).

To determine the substrate specificity of the induced [^{3}H]TPP uptake system of SLC44A4-expressing ARPE19 cells, we assessed the ability of unlabeled TPP, its structural analogs, *i.e.* free thiamine and TMP, as well as that of the unrelated nucleotides (ADP and ATP), carboxylic anions (butyrate and succinate), and nucleotide derivatives (FMN and FAD) (all at 200 μM) to affect the initial rate of [^{3}H]TPP (0.3 μM) uptake. The results (Fig. 3*D*) demonstrated that unlabeled TPP caused an almost complete inhibition (~98%) in [^{3}H]TPP uptake. In contrast, the other compounds tested showed either no (or little) effect. Because the TPPT system was originally assigned to the CTL family of proteins (24), we also examined the effect of a high concentration of choline (1 mM) on the initial rate of [^{3}H]TPP (0.3 μM) uptake by SLC44A4-expressing ARPE19 cells. The results (Fig. 3*D*) showed choline to have no effect on [^{3}H]TPP uptake by the induced system, further indicating that SLC44A4 is not a choline transporter.

We also determined the kinetic parameters of the TPP-induced system in SLC44A4-expressing ARPE19 cells. This was done by examining TPP uptake as a function of concentration (0.3–3.0 μM). The results (Fig. 3*E*) showed TPP uptake by the induced system to include a saturable component with kinetic parameters of 0.17 ± 0.064 μM for the apparent K_m and 54.56 ± 3.12 pmol (mg protein/3 min) for V_{max}. Collectively, the find-

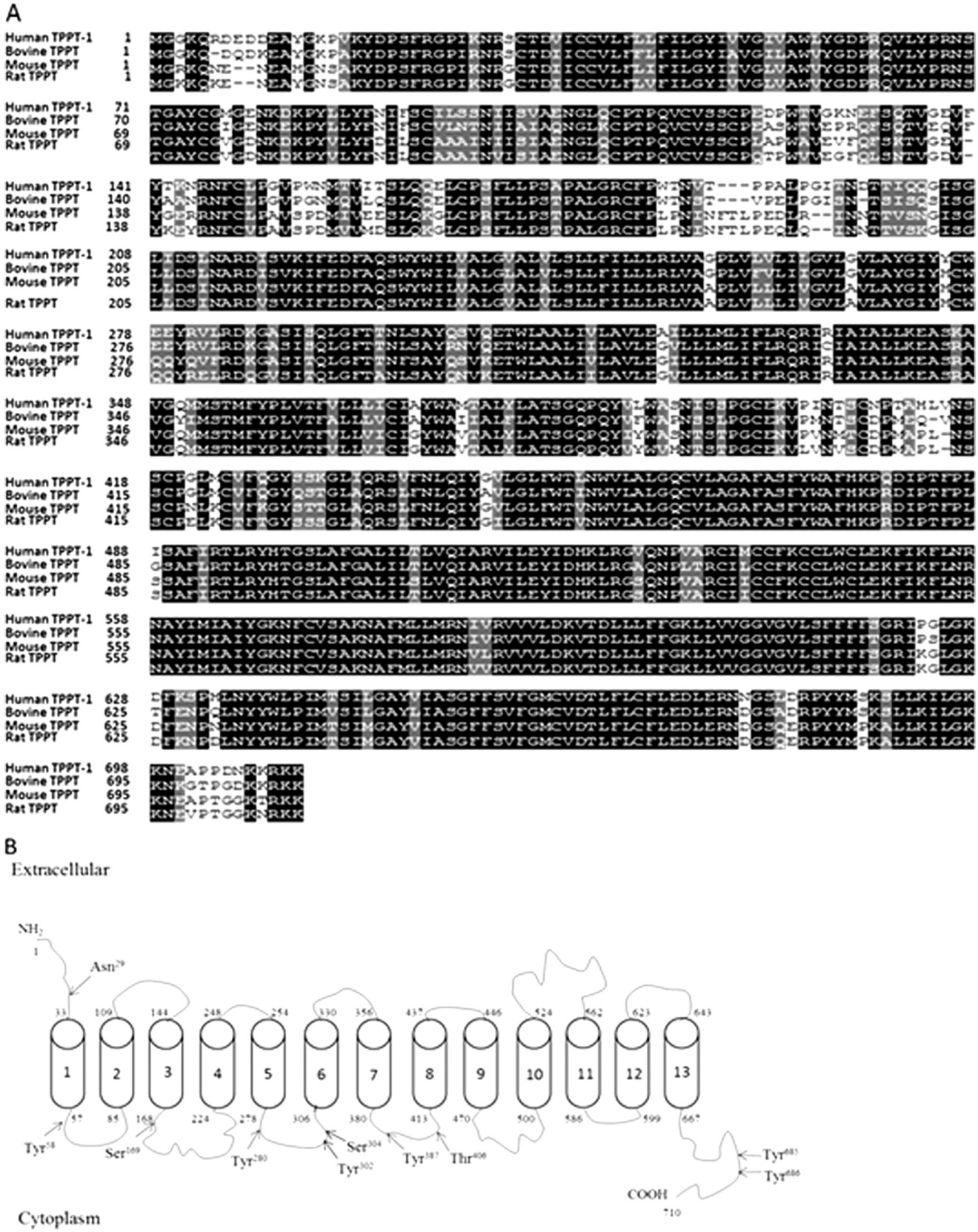

FIGURE 2. **Structural characteristics of hTPPT-1.** *A*, comparison of the deduced amino acid sequence of hTPPT-1 with those of bovine, mouse, and rat TPPT. Sequences of identity and similarity are shown in *black* and *gray*, respectively. *B*, membrane topology of hTPPT-1. By SOSUI, hTPPT-1 is predicted to have 13 potential transmembrane domains with NH_2 and COOH ends oriented outside and inside, respectively. The *arrows* indicate the location of potential *N*-glycosylation sites by the NetNGlyc1.0 server and potential sites of phosphorylation by the kinase prediction algorithm group-based prediction system (GPS) 2.1. A high threshold of GPS was chosen, with false positive predictions of 2 and 4% for Ser/Thr kinases and Tyr kinases, respectively.

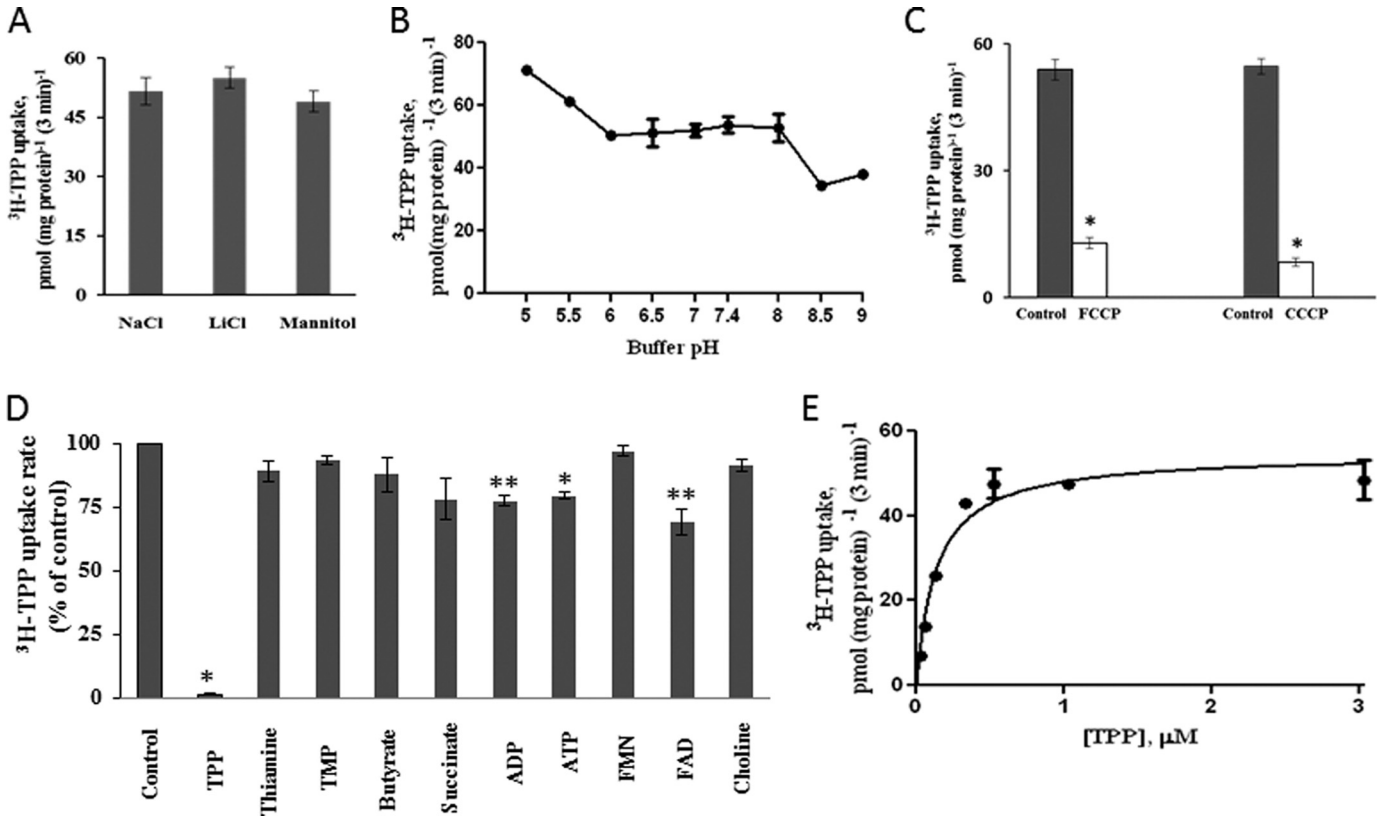

FIGURE 3. **Characteristics of the hTPPT-1-specific TPP uptake process by ARPE19 cells transiently transfected with hTPPT-1.** *A*, effect of Na^+ replacement on the initial rate of TPP uptake. Cells were incubated at 37 °C in Krebs-Ringer buffer (pH 7.4). NaCl (133 mM NaC) was replaced as indicated. [^{3}H]TPP (0.3 μM) was added to the incubation medium at the onset of incubation, and uptake was measured after 3 min of incubation. Data are mean ± S.E. of six to nine separate uptake determinations. *B*, effect of incubation buffer pH on the initial rate of TPP uptake. [^{3}H]TPP(0.3 μM) was added to the incubation medium (Krebs-Ringer buffer of varying pH) at the onset of incubation, and uptake was measured after 3 min of incubation. Data are mean ± S.E. of three to six separate uptake determinations. *C*, effect of FCCP and CCCP on the initial rate of TPP uptake. Cells were preincubated with FCCP or CCCP (both at 10 μM) for 20 min. Control cells were preincubated with ethanol or dimethyl sulfoxide, respectively. [^{3}H]TPP (0.3 μM) was added to the incubation medium (Krebs-Ringer buffer of pH 5.0, no protonophores) at the onset of incubation, and uptake was measured after 3 min of incubation. Data are mean ± S.E. of four to six separate uptake determinations. *, $p < 0.01$. *D*, effect of structural analogs of TPP and unrelated compounds on the initial rate of TPP uptake. Cells were incubated in uptake buffer (pH 7.4) at 37 °C in the presence of [^{3}H]TPP (0.3 μM) and an unlabeled compound (1 mM for choline and 200 μM for all other compounds). Uptake was measured after 3 min of incubation. Data are mean ± S.E. of six to 12 separate uptake determinations. *Control*, no unlabeled compound added. *, $p < 0.01$; **, $p < 0.05$. *E*, uptake of TPP as a function of substrate concentration. Cells were incubated in uptake buffer (pH 7.4) at 37 °C in the presence of different concentrations of TPP. Uptake was measured after 3 min of incubation (*i.e.* initial rate). Uptake by the carrier-mediated system was calculated as described under "Experimental Procedures." Data are mean ± S.E. of four to eight separate uptake determinations.

ings described above clearly indicate that SLC44A4 is a specific and high-affinity TPP uptake system.

Tissue and Cell Type Distribution of TPPT—The mRNA level of hTPPT was determined by quantitative RT-PCR using Human Major Tissue qPCR Panel II (OriGene) and our own RNA preparations from a variety of human cultured cell lines, including ARPE19 (retina), HuTu 80 (duodenum), HK-2 (kidney), HepG2 (liver), HeLa (cervix), Caco-2 (small intestine model), and NCM460 (colon) cells. The primers used in this study were specific for *SLC44A4* without discrimination between transcript variants. The results of the qRT-PCR analysis (Fig. 4, *A* and Fig. *B*) showed that the hTPPT mRNA is highly expressed in human colon and human colonic epithelial NCM460 cells with no or weak expression in other parts of gastrointestinal tract, *i.e.* stomach, duodenum, small intestine, and rectum. High expression of the SLC44A4 mRNA that is comparable with the colon was also detected in the prostate, trachea, and lung. Further studies, however, are needed to determine the physiological role of SLC44A4 in these tissues.

We also examined hTPPT expression at the protein level in the human colon and small intestine using purified proximal colonic AM and jejunal BBM preparations isolated from human organ donors. A Western blot analysis (Fig. 5) performed with the specific polyclonal anti-TPPT antibodies showed the presence of hTPPT protein (faint but reproducible immunoreactive bands of ~90–110 kDa; data on specificity of protein bands in colonic cells is also shown below under "Subcellular Localization of hTPPT") in the colonic AM but not in the jejunal BBM preparations. These observations further confirm the predominant hTPPT expression in the colon.

To gain more information regarding TPPT expression in distinct segments of colon, we performed qRT-PCR using total RNA isolated from mouse cecum, proximal colon, and distal colon (TPPT expression in mouse jejunum was studied in parallel) and specific mouse primers. The results (Fig. 6) showed a comparable level of mouse TPPT mRNA expression in all colonic segments tested, with very low expression in the jejunum.

Subcellular Localization of hTPPT—Plasma membrane localization of hTPPT was studied in human colonic epithelial NCM460 cells using a biotinylation approach followed by Western blot analysis. The results (Fig. 7, *lane 3*) showed the

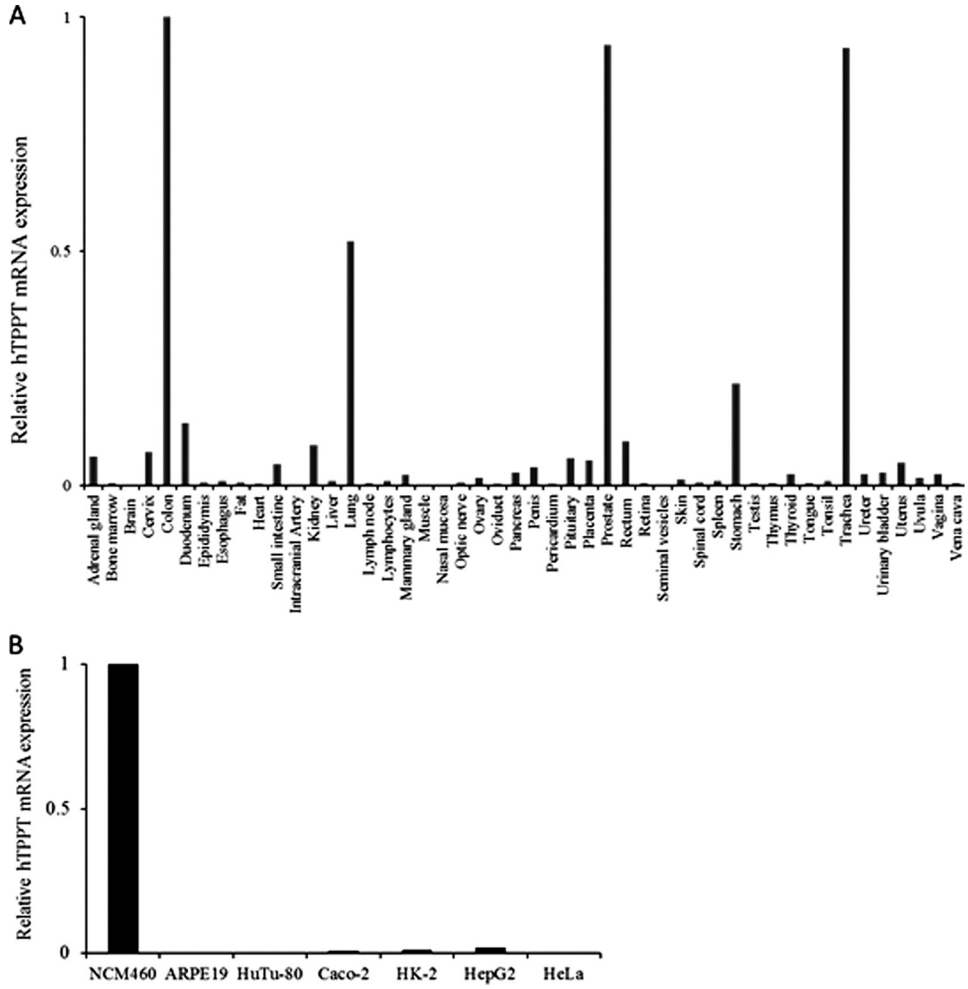

FIGURE 4. **Quantitative real-time PCR analysis of hTPPT mRNA expression in human tissues and human cell lines.** The Human Major Tissue qPCR Panel II, commercially available from OriGene (*A*), and total RNA of various human cell lines reverse-transcribed to cDNA (*B*) were used in qRT-PCR along with the gene-specific primers. Data normalized relative to GAPDH are from a representative set of experiments repeated twice with a similar result.

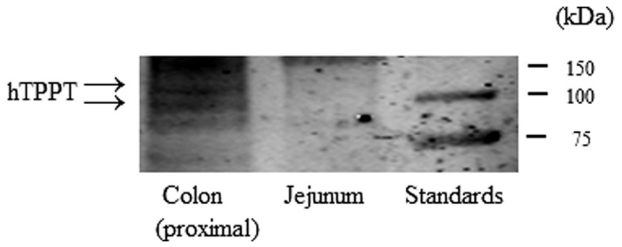

FIGURE 5. **Expression of hTPPT protein in human small and large intestine.** A Western blot analysis was performed using proximal colonic apical membrane vesicle and jejunal BBM vesicle preparations from human organ donors. Samples (equal amounts of 150 μg of total protein) were analyzed by immunoblotting using the polyclonal anti-hTPPT antibodies. The image is from a representative set of experiments.

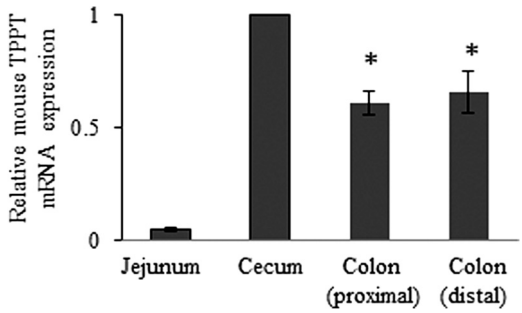

FIGURE 6. **Expression of mouse TPPT mRNA in various intestinal segments.** Total RNA was isolated from distinct segments of mouse intestine, and real-time quantitative PCR was performed. Data (mean ± S.E.), normalized relative to GAPDH, are from two mice, with RT-PCR performed three times. *, $p < 0.05$.

expression of hTPPT (single immunoreactive band of ~110 kDa) at the plasma membrane. The observed plasma membrane hTPPT seems to represent the glycosylated form of the protein (because the predicted molecular mass of hTPPT-1, *i.e.* the predominant colonic hTPPT isoform, is only 79.2 kDa). Interestingly, in whole NCM460 cell lysates, two distinct immunoreactive bands were clearly detected (Fig. 7, *lane 2*). In addition to an ~110-kDa band, a band of ~85–90 kDa was observed that most likely represents a non-glycosylated hTPPT (or a product of hTPPT posttranslational modification other than glycosylation).

Subcellular localization of hTPPT-1 was further examined in polarized renal epithelial MDCK cells transiently transfected with hTPPT-1-YFP. We used MDCK cells in this study because MDCK cells are a well suited model to study the polarized expression of membrane proteins. Confocal imaging of the living cells expressing hTPPT-1-YFP showed predominant apical plasma membrane localization of the protein (Fig. 8).

Isoforms of hTPPT in Human Colon Epithelial NCM460 Cells—The human *SLC44A4* gene, located on chromosome 6, spans about 16 kb and consists of 22 exons. As mentioned earlier, reference sequences of three alternatively spliced transcript variants of the human *SLC44A4* gene, *i.e.* transcript variants 1, 2, and 3, were found in the NCBI database. Transcript variant 1 (exon 2 skipped, use of exon 3) encodes the longest hTPPT isoform, isoform 1 (hTPPT-1), and is 710 amino acids in length. Transcript variant 2 (exons 2 and 7 skipped, use of exons 3 and 8) encodes hTPPT isoform 2 (hTPPT-2), which has the same N and C termini but is shorter (668 amino acids in length) than isoform 1 because of the loss of 42 amino acids from an alternate in-frame exon 7. Transcript variant 3 (exon 1 skipped, use of exon 2) encodes hTPPT isoform 3 (hTPPT-3), which represents the truncation of isoform 1 (only 634 amino acids in length, with the first 76 amino acids missing from the N terminus). We also examined the expression of these *SLC44A4* transcript variants by means of semiquantitative PCR in human colonic NCM460 cells and obtained results showing that only variants 1 and 3 are expressed (with no expression of variant 2 even after 35 cycles, data not shown). We also found the expression of variant 1 to be markedly higher than that of variant 3 (Fig. 9).

Because the hTPPT-3 variant is also expressed in NCM460 cells, we decided to examine its ability to transport TPP. For this, we cloned the ORF of this variant into the expression plasmid pFLAG-CMV-2 using mRNA from human colonic NCM460 cells and variant-specific primers, expressed the cDNA in ARPE19 cells, and performed a [^{3}H]TPP uptake assay. In parallel, uptake was determined in cells transiently transfected with hTPPT-1 (positive control). The results (Fig. 10) showed that the induction in [^{3}H]TPP uptake mediated by hTPPT-3 is similar to that mediated by hTPPT-1. These data indicate that hTPPT-3 is also a functionally active variant capable of transporting TPP.

Metabolism of TPP in Mouse Colonic Enterocytes—To gain insight into the metabolic fate of the TPP transported into colonocytes, we incubated [^{3}H]TPP (0.6 μM; 37 °C) with freshly prepared mouse colonic mucosal homogenate (~1 mg of total protein) for different periods of time, followed by determination of the forms of ^{3}H radioactivity by TLC (see "Experimental

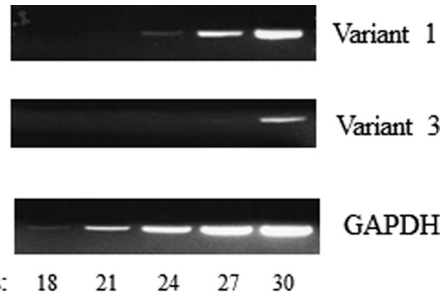

FIGURE 9. **Expression of SLC44A4 transcript variants in NCM460 cells.** Semiquantitative PCR was performed to estimate mRNA expression of *SLC44A4* transcript variants 1 and 3 (variant 2 is not expressed in these cells). The image is from a representative set of experiments with similar results.

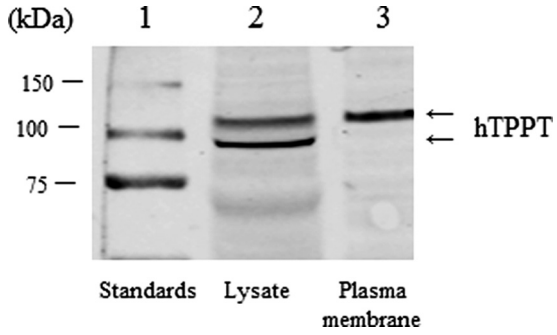

FIGURE 7. **Plasma membrane expression of hTPPT in colonic epithelial cells.** NCM460 cells were labeled with EZ-Link Sulfo-NHS-SS-Biotin, and biotinylated proteins were isolated with NeutrAvidin-agarose followed by Western blot analysis using the polyclonal anti-hTPPT antibodies. The image is representative of two separate sets of experiments with similar results.

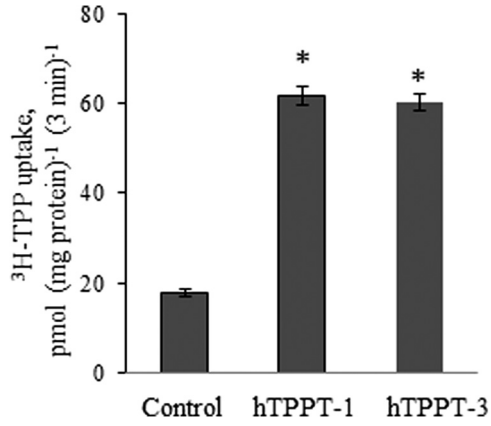

FIGURE 10. **Initial rate of [^{3}H]TPP uptake by ARPE19 cells transiently transfected with hTPPT-3.** Cells (48 h post-transfection) were incubated at 37 °C in Krebs-Ringer buffer (pH 7.4). [^{3}H]TPP (0.3 μM) was added to the incubation medium at the onset of incubation, and uptake was measured after 3 min of incubation (*i.e.* initial rate). Data are the mean ± S.E. of three to six separate uptake determinations. *Control*, cells transiently transfected with the empty pFLAG-CMV-2 vector. *, $p < 0.01$.

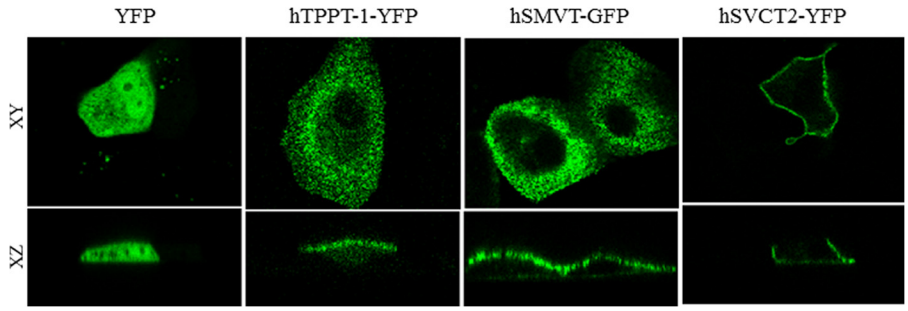

FIGURE 8. **Apical membrane targeting of hTPPT-1-YFP in polarized renal epithelial cells.** Targeting of YFP (vector alone), hTPPT-1-YFP, hSMVT-GFP (a known apical membrane marker (32)), and hSVCT2-YFP (a known basolateral membrane marker (33)) in MDCK cells in lateral (*xy*, *top row*) and axial (*xz*, *bottom row*).

Procedures"). The results showed that, after 1 h of incubation of TPP with the colonic mucosal homogenate, only ~39% of ^{3}H radioactivity was in the form of intact TPP, with the remaining ~45 and ~16% of radioactivity distributed between TMP and free thiamine, respectively. Longer (2 h) incubation of TPP with the colonic mucosal homogenate resulted in further TPP metabolism, with a distribution pattern of ^{3}H radioactivity as follows: ~29% of TPP, ~55% of TMP, and ~16% of free thiamine. These data suggest that considerable metabolism occurs in TPP following its uptake by colonocytes.

DISCUSSION

Our aim in this study was to determine the molecular identity of the system involved in TPP uptake we have identified recently, by functional means, in human colonocytes (16). This system appears to be involved in the uptake of the microbiota-generated TPP, which otherwise would be lost in the feces because of the inability of the colonocytes to convert this large, charged, and water-soluble molecule into free thiamine (colonocytes have little surface alkaline phosphatase activity (13–15)). We achieved our goal by bioinformatics analysis of the NCBI database, using as a query the recently identified TPP ABC transporter permease of the oral spirochete *T. denticola* (19). Our search has resulted in the identification of one candidate protein that showed significant similarity to the partial amino acid sequence of the query protein in regions predicted to participate in substrate recognition and binding (23). That protein is the product of the human *SLC44A4* gene, which so far has been considered as an uncharacterized multitransmembrane protein with an unknown function. The protein, however, has been classified as a member of the CTL family of proteins on the basis of some structural similarities and was given the name choline transporter-like protein 4 (CTL4) (reviewed in Ref. 24). The first member of the CTL family of transporters, *i.e.* CTL1 (a product of *SLC44A1* gene) was initially cloned from *Torpedo marmorata* (26). A CTL1-related protein was subsequently identified in mammals, followed by identification of other members of this family (*i.e.* CTL2–5, products of the *SLC44A2–5* genes) (24, 26, 27). CTL1 is, so far, the only member that demonstrates a choline transport function (24, 26, 27). In fact, evidence exists, from studies in yeast and nematodes, that suggests that paralogs of other members of SLC44A family are not choline transporters (28, 29).

We report here that the SLC44A4 system is in actuality a specific and high-affinity TPPT. We found three alternatively spliced variants of the human *SLC44A4* gene in the NCBI database. Because of our finding that SLC44A4 variant 1 is the predominant variant expressed in human colonic epithelial cells, we focused on this variant in our further investigations. We cloned SLC44A4 variant 1 from human colonic epithelial NCM460 cells and established its function as a specific and efficient TPPT by expression of its cDNA in human retinal pigment epithelial ARPE19 cells. Our functional characterization of the SLC44A4 system expressed in ARPE19 cells showed ^{3}H-TPP uptake by the induced carrier to be temperature- and energy-dependent but Na^+- independent in nature. TPP uptake by the induced system was detectable over a broad range of extracellular pH values, and although it did not display an obvious pH maximum, it was found to be slightly but significantly ($p < 0.01$) higher at an acidic pH of 5.0. Furthermore, a dissipation of the pH gradient by the proton ionophores FCCP and CCCP resulted in almost complete abolishment of TPP uptake by the induced system at pH 5.0, implying an important role for the pH gradient in the uptake process. With respect to these findings, the driving mechanism of TPPT is of particular interest. Taking into account the energy-dependent characteristics of this transporter, the absence of Na^+ involvement, and the importance of an outside-to-inside-directed H^+ gradient for the function of the transporter, it is possible to suggest that a TPP^--H^+ cotransport mechanism may be involved. Future studies are needed to confirm this suggestion.

The induced carrier was also found to be highly specific for TPP (unlabeled TPP caused an almost complete inhibition in induced [^{3}H]TPP uptake) but was not affected by free thiamine or TMP. It was also minimally affected by a host of other compounds that includes ADP, FMN, and butyrate. Of particular interest was the inability of a high concentration of choline (1 mM) to affect the uptake of [^{3}H]TPP by the induced carrier in the hTPPT-1-expressing ARPE19 cells. This finding further supports the conclusion that this system is not a choline transporter. We also determined the apparent K_m of the induced carrier and found it to be around 0.17 μM. This apparent K_m was very similar to the apparent K_m of the TPP uptake process found in intact human colonic NCM460 monolayers (around 0.16 μM) (16). All other major functional characteristics of energy dependence, Na^+ independence, a lack of an obvious extracellular pH maximum, and high specificity for TPP were also in agreement with those of the TPP transport system in NCM460 monolayers, strongly suggesting that TPPT is responsible for that transport system. At a physiological pH, TPP is negatively charged and can be considered an organic anion. We assessed the ability of known anion transport inhibitors such as probenecid and stilbene disulphonates, *i.e.* DIDS and SITS, to inhibit the hTPPT-1-specific uptake of [^{3}H]TPP, and, as expected, found that all of these compounds significantly inhibited uptake. It is interesting that amiloride, an organic cation, was also found to significantly inhibit the hTPPT-1-specific uptake of ^{3}H-TPP. This observation, together with the previously reported ability of amiloride to cause inhibition of uptake of free thiamine in a variety of cellular systems, including human intestinal epithelial cells (25), could indicate an important role of thiamine moiety in the TPP substrate molecule for recognition and/or binding of TPP with the hTPPT system. Further studies, however, are needed to test this possibility.

The hTPPT protein appears to be expressed in the human colon but not in the proximal small intestine. This conclusion was made on the basis of the results of the Western blot analysis using purified colonic AM and jejunal BBM vesicle preparations isolated from human organ donors. Similarly, a high expression of SLC44A4 mRNA was found in the human colon but not in the proximal small intestine (or in other parts of the gastrointestinal tract, like the stomach and rectum). These finding clearly indicated that the hTPPT is a predominantly colonic protein. We also investigated the cellular localization of the hTPPT protein in colonic epithelial cells. This was done by means of a cell surface biotinylation approach, with the results

showing clear plasma membrane localization (at this stage we could not differentiate between the hTPPT variant proteins because the antibodies used were raised against an antigenic peptide shared by all of them). The polarized expression of the hTPPT-1 protein in epithelial cells was also examined using a well established epithelial cell model for such investigations (the MDCK cell model), hTPPT-1-YFP, and a live-cell confocal imaging approach. The results showed predominant localization of the hTPPT-1 protein at the apical plasma membrane domain of these polarized epithelial cells.

We have shown previously that contact of TPP with human colonic epithelial cells does not affect the metabolic status of TPP (16), confirming the notion that colonocytes have little or no surface alkaline phosphatase (13–15). A question, however, exists as to what happens to the TPP molecule following its uptake into colonocytes. We addressed this issue by examining the metabolic forms of TPP (by TLC approach) following the incubation of [^{3}H]TPP with a homogenate of mouse colonic mucosa cells. The results showed a time-dependent and considerable TPP metabolism to free thiamine and TMP. On the basis of the above findings, we propose a model for TPP uptake by colonocytes in which TPP is first taken in by the TPPT system, with part of this TPP then being used for the metabolic needs of the colonocytes and the rest being metabolized to free thiamine and to TMP. Free thiamine could then move out of the cell across the basolateral membrane via the previously characterized THTR-1, which is expressed in colonocytes (12). As for TMP, this thiamine metabolite does exist in considerable amounts in the plasma (30), and, thus, it is possible that it can also leave the colonocyte via a yet to be identified transport system. Whether TPP itself can also cross the colonic basolateral membrane (knowing that there is some TPP in the plasma (31)) is not clear and requires further investigations.

In summary, findings of this study represent the first molecular identification and characterization of the membrane transport system involved in colonic TPP uptake. The identification of this system should assist in the performance of further investigations to understand the molecular regulation of the colonic TPP uptake process and how this process contributes toward overall thiamine nutrition, especially that of the local colonocytes.

REFERENCES

1. Berdanier, C. D. (1998) *Advanced Nutrition Micronutrients*, CRC Press, Boca Raton, FL
2. Bettendorff, L., and Wins, P. (2009) Thiamin diphosphate in biological chemistry. New aspects of thiamin metabolism, especially triphosphate derivatives acting other than as cofactors. *FEBS J.* **276,** 2917–2925
3. Said, H. M. (2011) Intestinal absorption of water-soluble vitamins in health and disease. *Biochem. J.* **437,** 357–372
4. Said, H. M. (2013) Recent advances in transport of water-soluble vitamins in organs of the digestive system. A focus on the colon and the pancreas. *Am. J. Physiol. Gastrointest. Liver Physiol.* **305,** G601–G610
5. Tanphaichirt, V. (1994) *Modern Nutrition in Health and Disease*, Lea and Febiger, New York
6. Victor, M., Adams, R. D., and Collins, G. H. (1989) *The Wernicke-Korsakoff Syndrome and Related Neurological Disorders due to Alcoholism and Malnutrition.* Davis, Philadelphia
7. Rindi, G., and Laforenza, U. (2000) Thiamine intestinal transport and related issues. Recent aspects. *Proc. Soc. Exp. Biol. Med.* **224,** 246–255
8. Arumugam, M., Raes, J., Pelletier, E., Le Paslier, D., Yamada, T., Mende, D. R., Fernandes, G. R., Tap, J., Bruls, T., Batto, J. M., Bertalan, M., Borruel, N., Casellas, F., Fernandez, L., Gautier, L., Hansen, T., Hattori, M., Hayashi, T., Kleerebezem, M., Kurokawa, K., Leclerc, M., Levenez, F., Manichanh, C., Nielsen, H. B., Nielsen, T., Pons, N., Poulain, J., Qin, J., Sicheritz-Ponten, T., Tims, S., Torrents, D., Ugarte, E., Zoetendal, E. G., Wang, J., Guarner, F., Pedersen, O., de Vos, W. M., Brunak, S., Doré, J., MetaHIT Consortium, Antolín, M., Artiguenave, F., Blottiere, H. M., Almeida, M., Brechot, C., Cara, C., Chervaux, C., Cultrone, A., Delorme, C., Denariaz, G., Dervyn, R., Foerstner, K. U., Friss, C., van de Guchte, M., Guedon, E., Haimet, F., Huber, W., van Hylckama-Vlieg, J., Jamet, A., Juste, C., Kaci, G., Knol, J., Lakhdari, O., Layec, S., Le Roux, K., Maguin, E., Mérieux, A., Melo Minardi, R., M'rini, C., Muller, J., Oozeer, R., Parkhill, J., Renault, P., Rescigno, M., Sanchez, N., Sunagawa, S., Torrejon, A., Turner, K., Vandemeulebrouck, G., Varela, E., Winogradsky, Y., Zeller, G., Weissenbach, J., Ehrlich, S. D., and Bork, P. (2011) Enterotypes of the human gut microbiome. *Nature* **473,** 174–180
9. Gurerrant, N. B., and Dutcher, R. A. (1932) The assay of vitamins B and G as influenced by coprophagy. *J. Biol. Chem.* **98,** 225–235
10. Gurerrant, N. B., Dutcher, R. A., and Brown, R. A. (1937) Further studies concerning formation of B vitamins in digestive tract of rat. *J. Nutr.* **13,** 305–315
11. Najjar, V. A., and Holt, L. E. (1943) The biosynthesis of thiamin in man and its implication in human nutrition. *J. Am. Med. Assoc.* **123,** 683–684
12. Said, H. M., Ortiz, A., Subramanian, V. S., Neufeld, E. J., Moyer, M. P., and Dudeja, P. K. (2001) Mechanism of thiamine uptake by human colonocytes. Studies with cultured colonic epithelial cell line NCM460. *Am. J. Physiol. Gastrointest. Liver Physiol.* **281,** G144–G150
13. Barrow, B. J., Ortiz-Reyes, R., O'Riordan, M. A., and Pretlow, T. P. (1989) *In situ* localization of enzymes and mucin in normal rat colon embedded in plastic. *Histochem. J.* **21,** 289–295
14. Czernobilsky, B., and Tsou, K. C. (1968) Adenocarcinoma, adenomas and polyps of the colon. Histochemical study. *Cancer* **21,** 165–177
15. Dawson, I., and Pryse-Davies, J. (1963) The distribution of certain enzyme systems in the normal human gastrointestinal tract. *Gastroenterology* **44,** 745–760
16. Nabokina, S. M., and Said, H. M. (2012) A high-affinity and specific carrier-mediated mechanism for uptake of thiamine pyrophosphate (TPP) by human colonic epithelial cells. *Am. J. Physiol. Gastrointest. Liver Physiol.* **303,** G389–G395
17. Brasitus, T. A., and Keresztes, R. S. (1984) Protein-lipid interactions in antipodal plasma membranes of rat colonocytes. *Biochim. Biophys. Acta* **773,** 290–300
18. Dudeja, P. K., Tyagi, S., Kavilaveettil, R. J., Gill, R., and Said, H. M. (2001) Mechanism of thiamin uptake by human jejunal brush-border membrane vesicles. *Am. J. Physiol. Cell Physiol.* **281,** C786–C792
19. Bian, J., Shen, H., Tu, Y., Yu, A., and Li, C. (2011) The riboswitch regulates a thiamine pyrophosphate ABC transporter of the oral spirochete *Treponema denticola*. *J. Bacteriol.* **193,** 3912–3922
20. Reidling, J. C., Nabokina, S. M., and Said, H. M. (2007) Molecular mechanisms involved in the adaptive regulation of human intestinal biotin uptake. A study of the hSMVT system. *Am. J. Physiol. Gastrointest. Liver Physiol.* **292,** G275–G281
21. Zhao, R., Gao, F., and Goldman, I. D. (2002) Reduced folate carrier transports thiamine monophosphate: an alternative route for thiamine delivery into mammalian cells. *Am. J. Physiol. Cell Physiol.* **282,** C1512–C1517
22. Wilkinson, G. N. (1961) Statistical estimation in enzyme kinetics. *Biochem. J.* **80,** 324–332
23. Shimamura, T., Weyand, S., Beckstein, O., Rutherford, N. G., Hadden, J. M., Sharples, D., Sansom, M. S., Iwata, S., Henderson, P. J., and Cameron, A. D. (2010) Molecular basis of alternating access membrane transport by the sodium-hydantoin transporter Mhp1. *Science* **328,** 470–473
24. Traiffort, E., O'Regan, S., and Ruat, M. (2013) The choline transporter-like family SLC44. Properties and roles in human diseases. *Mol. Aspects Med.* **34,** 646–654
25. Said, H. M., Ortiz, A., Kumar, C. K., Chatterjee, N., Dudeja, P. K., and Rubin, S. (1999) Transport of thiamine in human intestine. Mechanism and regulation in intestinal epithelial cell model Caco-2. *Am. J. Physiol.* **277,** C645–C651

26. O'Regan, S., Traiffort, E., Ruat, M., Cha, N., Compaore, D., and Meunier, F. M. (2000) An electric lobe suppressor for a yeast choline transport mutation belongs to a new family of transporter-like proteins. *Proc. Natl. Acad. Sci. U.S.A.* **97,** 1835–1840
27. Traiffort, E., Ruat, M., O'Regan, S., and Meunier, F. M. (2005) Molecular characterization of the family of choline transporter-like proteins and their splice variants. *J. Neurochem.* **92,** 1116–1125
28. Zufferey, R., Santiago, T. C., Brachet, V., and Ben Mamoun, C. (2004) Reexamining the role of choline transporter-like (Ctlp) proteins in choline transport. *Neurochem. Res.* **29,** 461–467
29. Mullen, G. P., Mathews, E. A., Vu, M. H., Hunter, J. W., Frisby, D. L., Duke, A., Grundahl, K., Osborne, J. D., Crowell, J. A., and Rand, J. B. (2007) Choline transport and de novo choline synthesis support acetylcholine biosynthesis in *Caenorhabditis elegans* cholinergic neurons. *Genetics* **177,** 195–204
30. Gangolf, M., Czerniecki, J., Radermecker, M., Detry, O., Nisolle, M., Jouan, C., Martin, D., Chantraine, F., Lakaye, B., Wins, P., Grisar, T., and Bettendorff, L. (October 25, 2010) Thiamine status in humans and content of phosphorylated thiamine derivatives in biopsies and cultured cells. *PLoS ONE* 10.1371/journal.pone.0013616
31. Tallaksen, C. M., Bøhmer, T., and Bell, H. (1992) Blood and serum thiamin and thiamin phosphate esters concentrations in patients with alcohol dependence syndrome before and after thiamin treatment. *Alcohol Clin. Exp. Res.* **16,** 320–325
32. Subramanian, V. S., Marchant, J. S., Boulware, M. J., Ma, T.Y., and Said, H. M. (2009) Membrane targeting and intracellular trafficking of the human sodium-dependent multivitamin transporter in polarized epithelial cells. *Am. J. Physiol. Cell Physiol.* **296,** C663–C671
33. Subramanian, V. S., Marchant, J. S., Reidling, J. C., and Said, H. M. (2008) *N*-Glycosylation is required for Na^+-dependent vitamin C transporter functionality. *Biochem. Biophys. Res. Commun.* **374,** 123–127